



ELSEVIER

Journal of Molecular Catalysis A: Chemical 119 (1997) 213–221

JOURNAL OF
MOLECULAR
CATALYSIS
A: CHEMICAL

Ethylene adsorption on the Cu(111) surface: DFT cluster studies

A. Michalak^{a,*}, M. Witko^b, K. Hermann^c

^a Department of Computational Methods in Chemistry, Faculty of Chemistry, Jagiellonian University, R. Ingardena 3, 30060 Cracow, Poland

^b Institute of Catalysis and Surface Chemistry, Polish Academy of Sciences, ul. Niezapominajek, 30239 Cracow, Poland

^c Fritz-Haber-Institut der MPG, Faradayweg 4-6, D-14195 Berlin, Germany

Received 21 July 1996; accepted 13 October 1996

Abstract

Experimental results for ethylene adsorbed at metal surfaces indicate major changes in the adsorbate structure, in particular an increased C–C distance, while the adsorption energy is found to be small. These findings can be explained by competitive adsorbate–substrate binding as evidenced in ab initio DFT cluster studies using a $\text{Cu}_7(4,3)\text{C}_2\text{H}_4$ cluster to simulate C_2H_4 adsorption on Cu(111). The calculations suggest that the adsorbate stabilizes in a cross-bridge orientation on Cu(111) where its C–C axis lies almost parallel to the surface and the two C centers point towards adjacent 3-fold fcc and hcp hollow sites. Further, the cluster results confirm the increased C–C distance of the adsorbate and predict bending of its CH_2 ends near the surface where the latter has not been observed so far. The distortion of the adsorbate is combined with rehybridization resulting in C–C bond weakening and increased adsorbate–substrate coupling characterized by a Dewar–Chatt–Duncanson type donation scheme.

Keywords: Copper; Adsorption; Ethene

1. Introduction

Small organic adsorbates play an important role as intermediates in many catalytic reactions near substrate surfaces, such as e.g. those connected with fossil fuel processing (see e.g., Ref. [1]). A full quantitative description of most of these processes is still lacking. However, the dehydrogenation of ethylene to yield acetylene on the Ni(111) surface serves as an example where surface science techniques have provided results which can be used to deduct the reaction

path on a microscopic scale. Recent photoelectron diffraction (PED) experiments [2,3] show that ethylene, adsorbed on Ni(111) at 120 K, stabilizes with its C–C axis almost parallel to the surface where the C centers bridge adjacent nearest neighbor Ni sites at the surface (top orientation, di- σ binding type). Heating the system results in dehydrogenation of the adsorbed ethylene to acetylene which occupies a different site and stabilizes in a cross-bridge orientation with the C–C axis parallel to the surface and C centers pointing towards adjacent fcc and hcp hollow sites. Both, C_2H_4 and C_2H_2 are found to be weakly bound to the surface whereas their geometry is changed substantially. In both

* Corresponding author.

molecules the C–C distance is increased by 0.26 Å for C₂H₄ and by 0.24 Å for C₂H₂. This C–C elongation due to adsorption has also been reported in PED measurements on Cu(111) + C₂H₂ [2–4], in surface extended X-ray adsorption fine structure (SEXAFS) measurements [5] on Cu(100) + C₂H₄, and in theoretical studies on Ni(110) + C₂H₄ [6]. The location of hydrogens in the adsorbates could not be observed by the experiments as a result of their small scattering cross sections.

Recent theoretical cluster work on Cu(111) + C₂H₂ [7–9] and on Pd(111) + C₂H₂ [9] has shown that the adsorbate stabilizes at the substrate surface in a distorted geometry where the C–C distance is enlarged and the CH ends are bent with respect to the (linear) free molecule geometry. The adsorbate–substrate interaction was described by a competitive mechanism [7,8] where energy is required to distort the molecule and gained by the (increased) binding of the distorted molecule with the substrate. The latter can be characterized by rehybridization (sp → sp²) in the adsorbate and by a Dewar–Chatt–Duncanson type donation mechanism [10,11] which is well known from organometallic chemistry [12]. The cluster models were able to describe the experimentally verified adsorbate site and orientation as well as the increased C–C distance in Cu(111) + C₂H₂ adequately. This proves their reliability in determining geometric details of the adsorbate system and suggests their use in other electronically equivalent systems.

A comparison of the above experimental data on the C₂H₂ adsorbate structure at Cu(111) and Ni(111) surfaces yields very similar results which may suggest the same behavior for adsorbed C₂H₄ on the two surfaces. Thus, from the experimental results on Ni(111) + C₂H₄ [2,3] one would expect for the Cu(111) + C₂H₄ system that the adsorbate stabilizes also in a top (di-σ binding) orientation where the C centers bridge adjacent nearest neighbor Cu sites. Since for the Cu(111) + C₂H₄ system structure parameters have not been measured so far, theoret-

ical predictions of the adsorbate geometry are highly desirable. Therefore, we have calculated geometric and electronic properties of the Cu(111) + C₂H₄ adsorbate system based on a small Cu₇(4,3)C₂H₄ cluster model. The electronic structure of the cluster is described by the density functional theory (DFT) method using a local spin density approximation (LSDA) for electron exchange and correlation. This work extends our previous cluster study on the Cu(111) + C₂H₂ adsorbate system [7,8] and the emphasis is on binding geometries while quantitative discussions of the adsorption energetics will be given only briefly.

The C₂H₄ adsorbate orientation on Cu(111) suggested by the calculations is analogous to that found in recent cluster studies on the Cu(111) + C₂H₂ system [7,8]. The adsorbate stabilizes in a cross-bridge orientation with the C–C axis parallel to the surface and C centers pointing towards adjacent fcc and hcp hollow sites. Thus, the C₂H₄ seems to orient itself differently on Cu(111) as compared to Ni(111) where the top (di-σ binding) orientation was observed in PED experiments [2,3]. However, the calculated increase of the C–C distance in adsorbed versus free C₂H₄ is consistent with experimental findings on Ni(111) + C₂H₄ [2,3] and on Cu(100) + C₂H₄ [5] as well as with theoretical results from cluster studies on Ni(110) + C₂H₄ [6]. The calculations suggest further that both CH₂ ends of adsorbed C₂H₄ are bent by about 50°. This adsorbate distortion leads to rehybridization and results in C–C bond weakening and increased adsorbate–substrate binding. The latter can be characterized by a Dewar–Chatt–Duncanson type donation/back-donation scheme [10,11] involving the 6a' HOMO's and 7a' LUMO's of the adsorbate as well as Cu 3d, 4sp orbitals.

Section 2 gives details of the cluster geometry and of the methods used to calculate the electronic structure of the cluster models. Section 3 presents the numerical results and discussion while Section 4 summarizes conclusions from the present study.

2. Theoretical details

In this work we use a $\text{Cu}_7(4,3)$ substrate cluster of C_s symmetry, see Fig. 1, which forms a compact section of the ideal $\text{Cu}(111)$ surface with four atoms of the first and three atoms of the second layer. This cluster, with the Cu-Cu nearest neighbor distance, $d_{\text{Cu-Cu}} = 4.824$ bohr, taken from the bulk, is found to give a reliable description of electronic properties of different adsorbate systems at the $\text{Cu}(111)$ surface [7,9,13,14]. It seems, therefore, appropriate for the present purpose. Ethylene adsorption is described by a $\text{Cu}_7(4,3)\text{C}_2\text{H}_4$ cluster where the adsorbate geometry is optimized keeping the substrate part of the cluster frozen. Here two C_2H_4 adsorbate orientations are considered. In a first orientation, the adsorbate is placed with its C-C axis at the C_s mirror plane of the substrate cluster, see left part of Fig. 1, where the adsorbate geometry starts from the planar free molecule ($d_{\text{C-C}} = 2.505$ bohr, $d_{\text{C-H}} =$

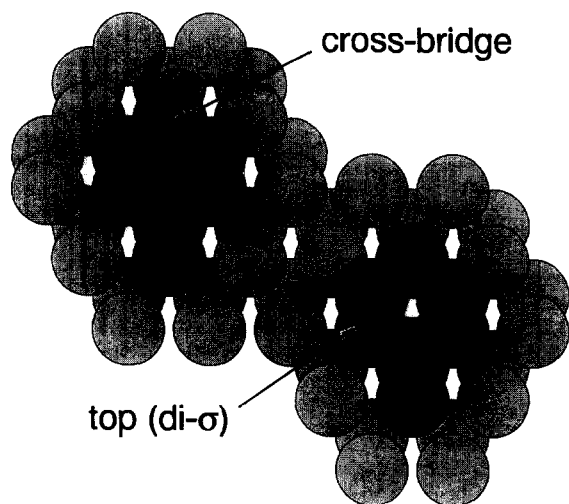


Fig. 1. Geometric structure of the $\text{Cu}_7(4,3)\text{C}_2\text{H}_4$ clusters used in the present study. In the first geometry, labeled 'cross-bridge' (left cluster), the C_2H_4 adsorbate bends over a $\text{Cu}(111)$ bridge site with its two C centers pointing towards adjacent fcc and hcp hollow sites of the substrate. In the second symmetry, labeled 'top (di- σ)' (right cluster), the C-C axis of C_2H_4 bridges a Cu-Cu nearest neighbor pair at the substrate surface. The very light balls in the figure represent Cu substrate atoms (not included in the clusters) which are meant to illustrate the $\text{Cu}(111)$ surface geometry.

2.022 bohr) bending symmetrically over a $\text{Cu}(111)$ bridge site (geometry labeled 'cross-bridge' in Fig. 1) and is optimized allowing all adsorbate centers to rearrange such that the C_s mirror plane is conserved. This is analogous to the optimization performed for the $\text{Cu}_7(4,3)\text{C}_2\text{H}_2$ cluster in a previous study [7,8]. In the second orientation, the adsorbate is placed with its C-C axis parallel to a Cu-Cu nearest neighbor pair at the substrate surface, see right part of Fig. 1, where the adsorbate geometry starts again from the planar free molecule with its C centers above the respective Cu centers (orientation labeled 'top (di- σ)' in Fig. 1) and is optimized allowing all adsorbate centers to rearrange such that C_s mirror plane symmetry is conserved.

The electronic structure and derived properties of the clusters are obtained with the ab initio density functional theory (DFT) method (see [15]; for the present calculations the DeMon program system was used. DeMon was developed by A. St-Amant and D. Salahub (University of Montreal) and is available from these authors) using the local spin density approximation (LSDA) for exchange and correlation based on the Vosko-Wilk-Nusair functional [16]. While the use of LSDA is known to yield poor binding energies for many molecular systems geometric quantities are always found to agree quite well with experiment [15] which justifies the use of LSDA for the present purpose. Gradient corrected exchange-correlation functionals are not expected to affect overall conclusions from the present work. The basis sets of contracted Gaussian orbitals (CGTO's) are all-electron type and taken from free atom DFT optimization [17]. The symmetry group of $\text{Cu}_7(4,3)\text{C}_2\text{H}_4$ is described by C_s , see Fig. 1, and all electronic states are calculated based on C_s symmetry even if their proper symmetry is higher. As an illustration we mention the isolated C_2H_4 adsorbate molecule which is characterized, apart from C_s , by D_{2h} (planar geometry) and by C_{2v} (bent geometry). The ground state configuration is described alternatively as

${}^1A'(6a'^2 2a''^2)$ in C_s , as ${}^1A_g(3a_g^2 2a_u^2 1b_{3u}^2 1b_{2g}^2 1b_{2u}^2)$ in D_{2h} , and as ${}^1A_1(4a_1^2 2b_1^2 1b_2^2 1a_2^2)$ in C_{2v} symmetry where $6a'$ ($1b_{2u}$, $4a_1$) denotes the HOMO and $7a'$, ($1b_{3g}$, $2b_2$) denotes the LUMO.

3. Results and discussion

Table 1 summarizes the computed geometry results of the free C_2H_4 molecule and of the adsorbate cluster $Cu_7(4,3)C_2H_4$ together with experimental data for the $Ni(111) + C_2H_4$ adsorbate system [2]. The well known planar equilibrium geometry of free ethylene is reproduced by the present DFT calculations with interatomic C–C and C–H distances which are in good agreement with standard quantum chemical results (see e.g. Ref. [18]). For C_2H_4 approaching the $Cu_7(4,3)$ cluster in the top orientation, see right part of Fig. 1, the adsorbate–substrate interaction is found always repulsive with no local energy minimum indicating equilibrium near the surface. When C_2H_4 approaches the $Cu_7(4,3)$ cluster in the cross-bridge orientation, see left part of Fig. 1, the adsorbate stabilizes above the Cu surface with its molecular geometry changed considerably with respect to that of free C_2H_4 . The DFT results of Table 1 yield a local equilibrium where the C–C axis

points parallel to the surface with a perpendicular C–Cu surface distance of $z_{C-Cu} = 3.13$ bohr. The C–C distance of the C_2H_4 adsorbate, $d_{C-C} = 2.88$ bohr, is greatly increased with respect to that of the free molecule, $d_{C-C} = 2.52$ bohr, while differences in the C–H distances are negligible. Further, the CH_2 ends of the adsorbate are bent away from the surface. This can be quantified by bending angles of the CH_2 planes with respect to the surface plane, yielding 47° ($\theta(CCH_2) = 133^\circ$ near fcc site, $= 134^\circ$ near hcp site), which results in a non-planar molecule geometry.

While theoretical studies on the $Cu(111) + C_2H_4$ adsorbate system do not seem to exist so far LCGTO-LDF cluster studies on the $Ni(110) + C_2H_4$ adsorbate system using $Ni_{14}(C_2H_4)_2$ clusters [6] yield an increased C–C distance, $d_{C-C} = 2.66$ bohr, for the adsorbate and its CH_2 ends bending away from the surface in consistency with our findings. However, the changes between free C_2H_4 and the adsorbate reported in Ref. [6] are less pronounced than those of the present study. This must be due to the different adsorbate surface orientations yielding the top orientation on $Ni(110)$ with C_2H_4 stabilizing further away from the surface as opposed to the cross-bridge orientation on $Cu(111)$ found to be preferred in the present system.

The computed equilibrium geometry of adsorbed C_2H_4 is compared in Table 1 with experimental PED results on the $Ni(111) + C_2H_4$ adsorbate system [2] since experimental data for $Cu(111) + C_2H_4$ do not exist so far. The perpendicular C–Cu surface distances z_{C-Cu} of the DFT treatment for $Cu(111)$ are smaller by 14% (0.47 bohr) compared to the experimental result for $Ni(111)$. This is explained by the different adsorbate orientation on $Ni(111)$ which is identified as top (see right part of Fig. 1) in the experiment whereas in the present calculations for $Cu(111)$ the top orientation is excluded and the cross-bridge orientation is found to be preferred. The difference in C_2H_4 adsorption on $Cu(111)$ and $Ni(111)$ is not obvious but most likely due to different d electron participation in

Table 1

Theoretical geometries of free C_2H_4 and of C_2H_4 in the $Cu_7(4,3)C_2H_4$ cluster referring to the cross-bridge orientation of the adsorbate, see Fig. 1. The density functional theory (DFT) data are compared with experimental geometries derived from photoelectron diffraction on the surface system $Ni(111) + C_2H_4$ [2]. The table lists the perpendicular C–Cu distances with respect to the Cu surface, z_{C-Cu} , and the C–C and C–H distances of the free molecule/adsorbate, d_{C-C} and d_{C-H} . Angle $\theta(CCH_2)$ determines bending of the CH_2 plane with respect to the surface plane. The two entries for z_{C-Cu} and $\theta(CCH_2)$ refer to the C centers closest to the fcc and hcp hollow surface sites, respectively

	Free C_2H_4	C_2H_4 in $Cu_7(4,3)C_2H_4$	Experiment $Ni(111) + C_2H_4$
z_{C-Cu} (bohr)	—	3.125/3.125	(3.59 ± 0.04)
d_{C-C} (bohr)	2.522	2.877	(3.02 ± 0.34)
d_{C-H} (bohr)	2.078	2.094	—
$\theta(CCH_2)$ (°)	180.0	132.8/133.9	—

the surface binding as a result of the open shell $3d^9$ structure of Ni compared to closed shell $3d^{10}$ for Cu. The increased C–C equilibrium distance, $d_{C-C} = 2.88$ bohr, found for $Cu_7(4,3)C_2H_4$ differs from the experimental PED result for $Ni(111) + C_2H_4$, $d_{C-C} = 3.02 \pm 0.34$ bohr, by less than 5% and lies within the experimental error bars. This suggests that the C–C distance is affected only little by the detailed surface orientation of the C_2H_4 adsorbate which is confirmed by surface extended X-ray-absorption fine-structure (SEXAFS) measurements on $Cu(100) + C_2H_4$ [5]. These measurements find an increased C–C distance, $d_{C-C} = 2.78 \pm 0.14$ bohr, for the adsorbate which lies within the range of the PED data for $Ni(111) + C_2H_4$ [2] and agrees with the present theoretical $Cu(111) + C_2H_4$ result. Calculated C–H distances and bending angles $\theta(CCH_2)$ of the C_2H_4 adsorbate cannot be compared with experimental data so far since hydrogen positions have not been measured by PED nor by SEXAFS [2,5]. However, bending of the CH_2 ends in the adsorbate seems to be of importance for the adsorbate–substrate binding which makes an experimental determination of d_{C-H} and $\theta(CCH_2)$ highly desirable.

The sizable restructuring of the C_2H_4 molecule upon adsorption on $Cu(111)$ is accompanied by a rather small adsorption energy as found in the experiment [2]. This is indicative of a competitive surface binding scheme where the adsorption energy is subdivided conceptually into contributions from two competing effects, (1) the distortion of the molecule by adsorption which requires energy (distortion energy), and (2) the binding of the distorted molecule near the substrate surface which gains energy. Both contributions must be of similar magnitude with (2) being slightly larger than (1) such that overall the adsorbate binds weakly to the surface. A first estimate of the distortion energy can be obtained from total energy calculations on C_2H_4 by itself using different geometries. The present DFT calculations yield a total energy of C_2H_4 in the (distorted) adsorbate geometry, obtained

for the $Cu_7(4,3)C_2H_4$ cluster, which lies 1.9 eV above that of the planar free molecule.

The geometric distortion of the adsorbate is intimately connected with changes in its electronic structure which can be rationalized by a simple rehybridization concept. In hydrocarbon chemistry the electronic structure of (planar) ethylene, C_2H_4 , is described by a C=C double bond and C– H_2 binding derives from sp^2 hybridization near the carbon centers while ethane, C_2H_6 , is described by a C–C single bond and C– H_3 binding due to sp^3 hybridization. Therefore, distorting the C_2H_4 molecule by bending its CH_2 ends to yield the adsorbate geometry may be viewed conceptually as creating an incomplete C_2H_6 molecule (with one hydrogen missing on each side) in its genuine geometry. This would lead to an effective transition from a C–C double to a weaker single bond and from sp^2 to sp^3 hybridization near the carbon centers of distorted C_2H_4 . The resulting sp^3 hybrid orbitals are not fully saturated making the C centers of C_2H_4 available for binding with the metal surface. On the other hand, C–C bond weakening in C_2H_4 due to rehybridization must lead to an increased C–C bond distance. The actual d_{C-C} value of adsorbed C_2H_4 determined by the present cluster study and from experiments [2] is consistent with the above interpretation. Typical distance values [19] obtained for carbon double ($d_{C-C} = 2.56$ bohr) and single bonds ($d_{C-C} = 2.92$ bohr) suggest that the C–C bond in adsorbed C_2H_4 ($d_{C-C} = 2.9$ – 3.0 bohr) may be better characterized as a single than a double bond.

Binding of the distorted C_2H_4 adsorbate with the Cu substrate surface can be described in detail by orbital and population analyses of the adsorbate cluster. Fig. 2 shows contour plots of the highest occupied orbital (HOMO) $6a'$ ($1b_{2u}$, $4a_1$) and of the lowest unoccupied orbital (LUMO) $7a'$ ($1b_{3g}$, $2b_2$) of C_2H_4 along a mirror plane containing its two carbon centers. In planar C_2H_4 the HOMO (bottom left plot, note that the contour plane is perpendicular to the molecular plane) is described by a bonding

combination of 2p functions at the two C centers and contributes to the C–C double bond in free ethylene. If the CH₂ ends on both sides of the molecule are bent and the C–C distance increased to reflect the C₂H₄ adsorbate geometry the HOMO (bottom right plot) admixes C 2sp character such that its lobes at the C centers become asymmetric accumulating more charge at the side adjacent to the Cu substrate. This can be connected with the sp² to sp³ rehybridization described above and allows the HOMO of the adsorbing C₂H₄ to easily mix with Cu 3d and 4sp orbitals resulting in a charge transfer (donation) from the adsorbate to the substrate. The charge transfer is partially compensated by a back-donation effect where Cu 3d and 4sp ad-

mix contributions of the adsorbate LUMO thereby transferring charge from the metal to the substrate. The LUMO which is described in the free C₂H₄ as an anti-bonding combination of C 2p functions (top left plot) is also modified in the adsorbate geometry by additional C 2sp contributions (top right plot) which increase its charge at the side adjacent to the Cu substrate and enhances its availability for back-donation. The present donation/back-donation scheme is well known from the theory of hydrocarbon–metal binding in complexes [12] and at surfaces [7,9,20–22] and is recognized as the Dewar–Chatt–Duncanson mechanism [10,11]. It is completely analogous to the Blyholder scheme proposed for CO–metal binding in carbonyls

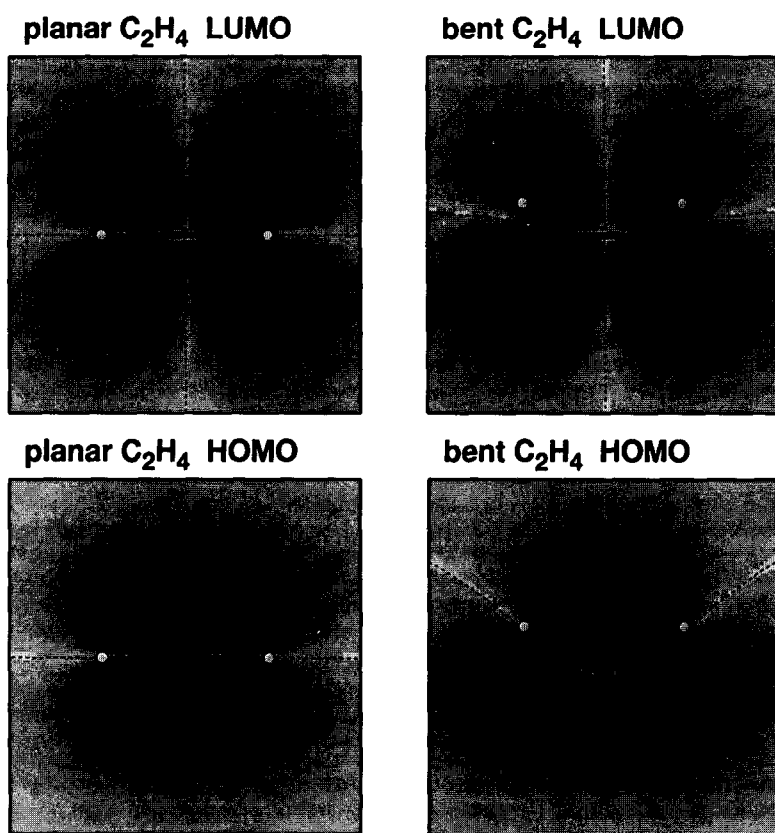


Fig. 2. Shaded contour plots of the highest occupied orbital (HOMO), 6a' (1b_{2u}, 4a₁), and of the lowest unoccupied orbital (LUMO), 7a' (1b_{3g}, 2b₂) of C₂H₄ in its free molecule (planar) and adsorbate (bent) geometry. The contour plane forms a mirror plane of the molecule containing its two C centers (marked by black dots) and lies perpendicular to the atom plane of free C₂H₄. The H centers (marked by circles) are placed symmetrically above and below the contour plane. Full (dashed) lines refer to positive (negative) wave function values with contours ranging from -0.28 au to $+0.28$ au (1 au = 1 e/bohr³) with equidistant increments of 0.04 au. The shaded overlay sketches the electron density of each orbital.

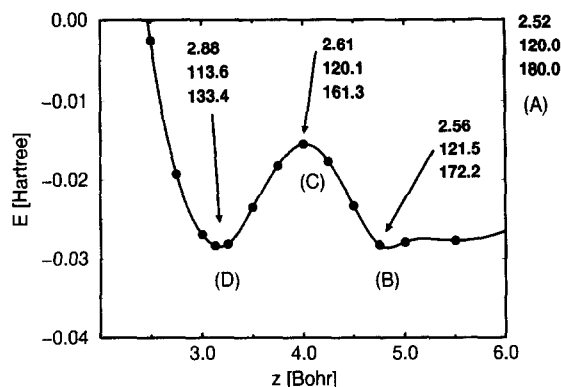


Fig. 3. Interaction curve of the $\text{Cu}_7(4,3)\text{C}_2\text{H}_4$ system, see text. The interaction energy $E(z)$, given as a function of the perpendicular adsorbate distance z , refers to C_2H_4 approaching with its C–C axis parallel to the surface and its molecular geometry optimized for each z value. Example results of the adsorbate geometry are added for four typical distances, (A)–(D) where each triple of numbers gives (from top to bottom) the optimized C–C distance (in bohr), the angle $\angle(\text{HCH})$, and the bending angle $\theta(\text{CCH}_2)$ (in degrees).

and at surfaces [23,24]. Clearly, the present discussion of C_2H_4 –Cu binding can only be qualitative and needs to be substantiated by more quantitative analyses [25,26]. However, we believe that the essential binding contributions become obvious already from the orbital plots of Fig. 2.

The actual adsorption mechanism of C_2H_4 on Cu(111) can be rather complex and may involve activation barriers along the adsorption path. As an example, Fig. 3 shows the total energy curve $E(z)$ of the $\text{Cu}_7(4,3)\text{C}_2\text{H}_4$ cluster for an adiabatic model path where the C_2H_4 molecule is approaching Cu_7 with its C–C axis parallel to the surface in a cross-bridge orientation. For each distance z between the C–C axis and the Cu surface the adsorbate geometry has been optimized to reflect the influence by the adsorbate–substrate interaction. Example results of the adsorbate geometry are added to the energy curve for four typical distances, denoted (A)–(D), where each triple of numbers gives (from top to bottom) the optimized C–C distance (in bohr), the angle $\angle(\text{HCH})$, and the bending angle $\theta(\text{CCH}_2)$ (in degrees). For infinite separation z between adsorbate and sub-

strate, point (A) defining the total energy zero, the molecule assumes its planar geometry ($\angle(\text{HCH}) = 120^\circ$, $\theta(\text{CCH}_2) = 180^\circ$). At finite distances, between points (A) and (B) ($z = 4.8$ bohr), there is a weak attractive Cu– C_2H_4 interaction. Here the molecule bends its CH_2 ends by 8° and increases its C–C separation by 0.04 bohr over a large distance range. For smaller distances z the molecular distortion sets in much more rapidly. Between points (B) ($z = 4.8$ bohr) and (C) ($z = 4.0$ bohr), the CH_2 bending and C–C distance grow by 11° and 0.05 bohr, respectively. Here the increase in distortion energy cannot be compensated by the energy gain due to Cu– C_2H_4 binding, resulting in a repulsive Cu– C_2H_4 interaction and an energy barrier which is reached at point (C). The energy balance is reversed between points (C) ($z = 4.0$ bohr) and (D) ($z = 3.12$ bohr) leading to adsorbate–substrate attraction and the adsorbate geometry change becomes most dramatic ($\theta(\text{CCH}_2)$ grows by 28° , $d_{\text{C-C}}$ by 0.27 bohr). Finally, the global energy minimum is reached at point (D) where the C_2H_4 distortion is largest with angles $\angle(\text{HCH}) = 114^\circ$ and $\theta(\text{CCH}_2) = 133^\circ$ getting close to those of the tetrahedral sp^3 geometry ($\angle(\text{HCH}) = 109.47^\circ$, $\theta(\text{CCH}_2) = 125.26^\circ$). The interaction curve of Fig. 3 with its two minima rather close in energy could suggest a precursor state of the adsorbate at a rather large distance (point (C)) in addition to the minimum at point (D).

However, this result may be an artifact due to the restricted adsorption path and the present energy barrier, 0.37 eV from Fig. 3, could be lowered considerably if more general paths are considered.

4. Conclusions

The present DFT calculations on C_2H_4 and $\text{Cu}_7(4,3)\text{C}_2\text{H}_4$ can give useful information on the geometric structure and adsorbate–substrate bond formation of the Cu(111) + C_2H_4 adsor-

bate system which has not yet been examined in its detailed geometry by experiments. The calculations yield a C_2H_4 adsorbate orientation which is identical to that of the $Cu(111) + C_2H_2$ system found both in theoretical [7–9] and experimental [2–4] studies. The adsorbate stabilizes over a bridge site with its C–C axis almost parallel to the surface and the two C centers pointing towards adjacent 3-fold fcc and hcp hollow sites (cross-bridge orientation). The top orientation, favored by experimental results from PED studies on $Ni(111) + C_2H_4$ [2] is excluded by the calculations. In the calculations the C–C distance of the adsorbate is greatly increased over that of free C_2H_4 which is consistent with experimental findings of PED studies on $Ni(111) + C_2H_4$ [2], with SEXAFS studies on $Cu(100) + C_2H_4$ [5]. Further, the calculations predict that both CH_2 ends of adsorbed C_2H_4 are bent (by about 50°) pointing away from the surface which has not yet been found experimentally but is in qualitative agreement with cluster studies for $Ni(110) + C_2H_4$ [6].

The adsorbate–substrate interaction is described by a competitive binding scheme consisting conceptually of two contributions, the geometric distortion of the molecule by adsorption which requires energy, and the binding of the distorted molecule near the substrate surface which gains energy. Both contributions must be of similar magnitude such that overall the adsorbate binds weakly to the surface. The distortion energy is roughly estimated from DFT calculations on the free C_2H_4 molecule to yield 1.9 eV. Further, binding of the distorted molecules with the surface can be described by a Dewar–Chatt–Duncanson [10,11] donation/back-donation mechanism involving the $6a'$ HOMO's and $7a'$ LUMO's of C_2H_4 as well as Cu 3d, 4sp orbitals.

More detailed calculations including a larger set of substrate clusters differing in size and shape [13,14,24] as well as more complex geometry variations of the adsorbate are needed to confirm the present findings. This concerns, in particular, details of the adsorption process and

possible precursor states which involve studies of many different adsorption paths. However, the present work confirms that small hydrocarbon adsorbate systems are interesting examples where major geometry changes of the adsorbate are combined with overall weak adsorption which can be explained by a competitive binding scheme.

Acknowledgements

This work was funded in parts by the Deutsche Forschungsgemeinschaft and Fonds der Chemischen Industrie. Further support was based on grant No. 3T09A 11708 from the State Committee for Scientific Research of Poland.

References

- [1] B. Delmon and J.T. Yates (Editors), *Surface Science and Catalysis*, Vol. 45, Elsevier, Amsterdam, 1989.
- [2] S. Bao, P. Hofmann, K.M. Schindler, V. Fritzsche, A.M. Bradshaw, D.P. Woodruff and M.C. Asensio, *J. Phys.: Condens. Matter* 6 (1994) L93.
- [3] S. Bao, P. Hofmann, K.M. Schindler, V. Fritzsche, A.M. Bradshaw, D.P. Woodruff, C. Casado and M.C. Asensio, *Surf. Sci.* 323 (1995) 19.
- [4] S. Bao, K.-M. Schindler, P. Hofmann, V. Fritzsche, A.M. Bradshaw and D.P. Woodruff, *Surf. Sci.* 291 (1994) 295.
- [5] D. Arvanitis, L. Wenzel and K. Baberschke, *Phys. Rev. Lett.* 59 (1987) 2435.
- [6] M. Weinelt, W. Huber, P. Zebisch, H.-P. Steinrück, M. Pabst and N. Rösch, *Surf. Sci.* 271 (1992) 539.
- [7] K. Hermann and M. Witko, *Surf. Sci.* 337 (1995) 205.
- [8] K. Hermann, M. Witko and A. Michalak, *Z. Phys. Chem.*, in press.
- [9] A. Clotet and G. Pachioni, *Surf. Sci.* 346 (1996) 91.
- [10] M.J.S. Dewar, *Bull. Soc. Chim. France* 18 (1951) C79.
- [11] J. Chatt and L.A. Duncanson, *J. Chem. Soc.* (1953) 2939.
- [12] M.R. Albert and J.T. Yates, *The Surface Scientist's Guide to Organometallic Chemistry*, ACS Publishing, Washington 1987.
- [13] K. Hermann, M. Witko, L.G.M. Pettersson and P. Siegbahn, *J. Chem. Phys.* 99 (1993) 610.
- [14] M. Witko and K. Hermann, *J. Chem. Phys.* 101 (1994) 10173.
- [15] J.K. Labanowski and J.W. Anzelm (Editors), *Density Functional Methods in Chemistry*, Springer-Verlag, New York, 1991.
- [16] S.H. Vosko, L. Wilk and M. Nusair, *Can. J. Phys.* 58 (1980) 1200.

- [17] N. Godbout, D.R. Salahub, J. Andzelm and E. Wimmer, *Can. J. Phys.* 70 (1992) 560.
- [18] F. Hampel, in: P.V.R. Schleyer (Editor), *Theoretical Structures of Molecules in Landolt-Börnstein, New Series, Group II (Atomic and Molecular Physics)*, Vols. 22a/b, Springer, Berlin, 1994.
- [19] R.T. Morrison and R.N. Boyd, *Organic Chemistry*, 3rd Ed., Allyn and Bacon, Boston, 1999.
- [20] P. Geurts and A. van der Avoird, *Surf. Sci.* 102 (1981) 185.
- [21] P. Geurts and A. van der Avoird, *Surf. Sci.* 103 (1981) 416.
- [22] A.B. Anderson, *J. Am. Chem. Soc.* 99 (1977) 696.
- [23] G. Blyholder, *J. Phys. Chem.* 68 (1964) 2772.
- [24] K. Hermann, P.S. Bagus and C.J. Nelin, *Phys. Rev. B* 35 (1987) 9467.
- [25] P.S. Bagus, K. Hermann and C.W. Bauschlicher, *J. Chem. Phys.* 80 (1984) 4378.
- [26] P.S. Bagus, K. Hermann and C.W. Bauschlicher, *J. Chem. Phys.* 81 (1984) 1966.